



<b>Title</b>	<b>Effects of Ta incorporation in La<sub>2</sub>O<sub>3</sub> gate dielectric of InGaZnO thin-film transistor</b>
<b>Author(s)</b>	<b>QIAN, L; Lai, PT</b>
<b>Citation</b>	<b>Applied Physics Letters, 2014, vol. 104 n. 2, article no. 123505</b>
<b>Issued Date</b>	<b>2014</b>
<b>URL</b>	<b><a href="http://hdl.handle.net/10722/202931">http://hdl.handle.net/10722/202931</a></b>
<b>Rights</b>	<b>Copyright 2014 American Institute of Physics. This article may be downloaded for personal use only. Any other use requires prior permission of the author and the American Institute of Physics. The following article appeared in Applied Physics Letters, 2014, vol. 104 n. 2, article no. 123505 and may be found at <a href="http://scitation.aip.org/content/aip/journal/apl/104/12/10.1063/1.4869761">http://scitation.aip.org/content/aip/journal/apl/104/12/10.1063/1.4869761</a></b>

## Effects of Ta incorporation in La<sub>2</sub>O<sub>3</sub> gate dielectric of InGaZnO thin-film transistor

L. X. Qian, P. T. Lai, and W. M. Tang

Citation: [Applied Physics Letters](#) **104**, 123505 (2014); doi: 10.1063/1.4869761

View online: <http://dx.doi.org/10.1063/1.4869761>

View Table of Contents: <http://scitation.aip.org/content/aip/journal/apl/104/12?ver=pdfcov>

Published by the [AIP Publishing](#)

---

### Articles you may be interested in

[Comparison of structural and electrical properties of Lu<sub>2</sub>O<sub>3</sub> and Lu<sub>2</sub>TiO<sub>5</sub> gate dielectrics for  \$\alpha\$ -InGaZnO thin-film transistors](#)

[J. Appl. Phys.](#) **116**, 194510 (2014); 10.1063/1.4902518

[Low-cost Xe sputtering of amorphous In-Ga-Zn-O thin-film transistors by rotation magnet sputtering incorporating a Xe recycle-and-supply system](#)

[J. Vac. Sci. Technol. A](#) **32**, 02B105 (2014); 10.1116/1.4835775

[Investigation of tow-step electrical degradation behavior in a-InGaZnO thin-film transistors with Sm<sub>2</sub>O<sub>3</sub> gate dielectrics](#)

[Appl. Phys. Lett.](#) **103**, 033517 (2013); 10.1063/1.4816057

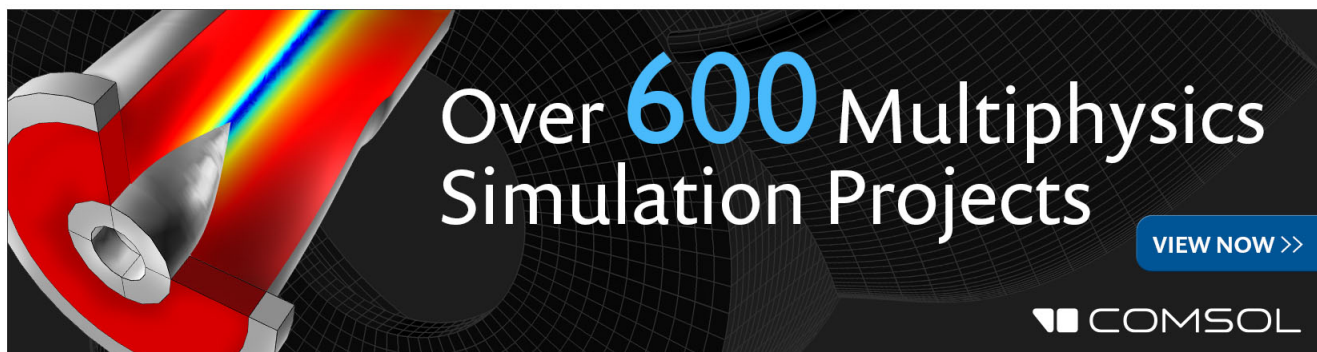
[Effect of hydrogen incorporation on the negative bias illumination stress instability in amorphous In-Ga-Zn-O thin-film-transistors](#)

[J. Appl. Phys.](#) **113**, 063712 (2013); 10.1063/1.4792229

[Investigating the degradation behavior caused by charge trapping effect under DC and AC gate-bias stress for InGaZnO thin film transistor](#)

[Appl. Phys. Lett.](#) **99**, 022104 (2011); 10.1063/1.3609873

---

The advertisement features a 3D cutaway of a mechanical part with a colorful stress or temperature distribution. The text 'Over 600 Multiphysics Simulation Projects' is prominently displayed in white and blue. A blue button with the text 'VIEW NOW >>' is located to the right. The COMSOL logo is in the bottom right corner.

Over **600** Multiphysics Simulation Projects

[VIEW NOW >>](#)

COMSOL

## Effects of Ta incorporation in $\text{La}_2\text{O}_3$ gate dielectric of InGaZnO thin-film transistor

L. X. Qian,<sup>1</sup> P. T. Lai,<sup>1,a)</sup> and W. M. Tang<sup>2</sup>

<sup>1</sup>Department of Electrical and Electronic Engineering, The University of Hong Kong, Pokfulam Road, Hong Kong

<sup>2</sup>Department of Applied Physics, The Hong Kong Polytechnic University, Hung Hom, Kowloon, Hong Kong

(Received 25 December 2013; accepted 17 March 2014; published online 26 March 2014)

The effects of Ta incorporation in  $\text{La}_2\text{O}_3$  gate dielectric of amorphous InGaZnO thin-film transistor are investigated. Since the Ta incorporation is found to effectively enhance the moisture resistance of the  $\text{La}_2\text{O}_3$  film and thus suppress the formation of  $\text{La}(\text{OH})_3$ , both the dielectric roughness and trap density at/near the InGaZnO/dielectric interface can be reduced, resulting in a significant improvement in the electrical characteristics of transistor. Among the samples with different Ta contents, the one with a Ta/(Ta+La) atomic ratio of 21.7% exhibits the best performance, including high saturation carrier mobility of  $23.4 \text{ cm}^2/\text{V}\cdot\text{s}$ , small subthreshold swing of  $0.177 \text{ V}/\text{dec}$ , and negligible hysteresis. Nevertheless, excessive incorporation of Ta can degrade the device characteristics due to newly generated Ta-related traps. © 2014 AIP Publishing LLC. [<http://dx.doi.org/10.1063/1.4869761>]

Recently, amorphous InGaZnO (a-IGZO) thin-film transistors (TFTs) have been extensively explored for the application in various flat-panel displays.<sup>1,2</sup> Compared to conventional amorphous silicon or organic TFTs with a field-effect carrier mobility of  $\sim 1 \text{ cm}^2/\text{V}\cdot\text{s}$ ,<sup>3,4</sup> a-IGZO TFTs typically exhibit a mobility higher than  $10 \text{ cm}^2/\text{V}\cdot\text{s}$ ,<sup>5</sup> which can translate to higher switching speed for electronic devices. In addition, a-IGZO TFTs offer better uniformity in device characteristics compared with polycrystalline silicon TFTs and have more excellent transparency to visible light than all the silicon-based devices.<sup>6</sup> In order to reduce their operating voltage, high-k materials have been adopted as gate dielectric in a-IGZO TFTs.<sup>7,8</sup> Among them, rare-earth oxide  $\text{La}_2\text{O}_3$  is regarded as one of the most promising candidates due to its relatively high dielectric constant and large band gap ( $\sim 6 \text{ eV}$ ).<sup>9,10</sup> However,  $\text{La}_2\text{O}_3$  is hygroscopic, which can deteriorate both the dielectric constant and surface roughness of  $\text{La}_2\text{O}_3$  film due to the formation of hydroxide  $\text{La}(\text{OH})_3$ ,<sup>11</sup> and thus induce degradations in the electrical characteristics of a-IGZO TFTs.<sup>12</sup> Fortunately, the doping of other elements, for example, Y, was reported to be an effective method to suppress the moisture absorption of  $\text{La}_2\text{O}_3$  film.<sup>13</sup> In this work, the doping of Ta in  $\text{La}_2\text{O}_3$  film is proposed due to the fact that  $\text{Ta}_2\text{O}_5$  can exhibit both very high dielectric constant and excellent step coverage,<sup>14</sup> and accordingly the effects of Ta incorporation in  $\text{La}_2\text{O}_3$  gate dielectric of a-IGZO TFTs are investigated. Three samples of a-IGZO TFTs with different Ta/(Ta+La) atomic ratios are prepared while one sample with pure  $\text{La}_2\text{O}_3$  gate dielectric is also fabricated as the control sample.

Each sample was fabricated on a p-type (100) silicon wafer with a resistivity of  $0.01\text{--}0.02 \text{ }\Omega\cdot\text{cm}$  which acted as both the substrate and gate electrode. First, a 40-nm dielectric film was deposited by a sputtering system under a radio-frequency (RF) power supply for a ceramic target of  $\text{La}_2\text{O}_3$  and a direct-current (DC) supply for a metal target of Ta in a

mixed ambient of Ar plus  $\text{O}_2$ . The RF power was fixed at 40 W while the DC supply was set to be 0 A, 0.03 A, 0.04 A, and 0.05 A for sample  $\text{La}_2\text{O}_3$ , sample  $\text{LaTaO}_A$ , sample  $\text{LaTaO}_B$ , and sample  $\text{LaTaO}_C$ , respectively, so as to realize different atomic ratios of Ta/(Ta+La) in dielectric films. Second, an annealing treatment at  $400 \text{ }^\circ\text{C}$  in an  $\text{N}_2$  ambient for 30 min followed. Subsequently, the four samples received the deposition of a 60-nm a-IGZO active layer through RF sputtering from a ceramic target ( $\text{Ga}_2\text{O}_3$ :  $\text{In}_2\text{O}_3$ :  $\text{ZnO} = 1: 1: 1$ ). After that, a lift-off process was utilized to form the source/drain electrodes, which were composed of 20-nm Ti and 80-nm Au. The channel width (W) and channel length (L) were  $100 \text{ }\mu\text{m}$  and  $10 \text{ }\mu\text{m}$ , respectively. Finally, all the samples were annealed in a forming-gas ( $\text{N}_2$ :  $\text{H}_2 = 95: 5$ ) ambient at  $350 \text{ }^\circ\text{C}$  for 20 min so that the contact resistance of the source/drain electrodes was reduced. In addition, metal-insulator-semiconductor capacitor was also prepared beside each sample to monitor the gate-oxide capacitance per unit area ( $C_{\text{ox}}$ ). The current-voltage (I-V) curves of the TFTs were measured by a HP 4145B semiconductor parameter analyzer. Furthermore, the structural properties of the dielectric films were studied based on X-ray photoelectron spectroscopy (XPS) and atomic force microscopy (AFM).

Fig. 1 shows the XPS spectra of (a) La  $3d_{5/2}$  and (b) O  $1s$  core levels for the dielectric films. The binding energies have been corrected for sample charging effect with reference to the C  $1s$  line at  $285.0 \text{ eV}$ . Accordingly to the XPS result, the atomic ratio of Ta/(Ta+La) is 0%, 21.7%, 30.6%, and 69.1% for sample  $\text{La}_2\text{O}_3$ , sample  $\text{LaTaO}_A$ , sample  $\text{LaTaO}_B$ , and sample  $\text{LaTaO}_C$ , respectively. As shown in Fig. 1(a), the  $\text{La}_2\text{O}_3$  film exhibits an obvious shoulder at the high binding energy side of the La  $3d_{5/2}$  main peak, suggesting the presence of La-OH bond due to the moisture absorption of  $\text{La}_2\text{O}_3$ . Furthermore, the La  $3d_{5/2}$  peak of the  $\text{La}_2\text{O}_3$  film (located at  $834.7 \text{ eV}$ ) shifts to a higher binding energy compared to the ideal  $\text{La}_2\text{O}_3$  reference peak (located at  $834.0 \text{ eV}$ ) while being consistent with the reported peak for LaOOH film (located at  $834.8 \pm 0.2 \text{ eV}$ ) in peak location,<sup>15</sup> further revealing the

<sup>a)</sup>Electronic mail: laip@eee.hku.hk.

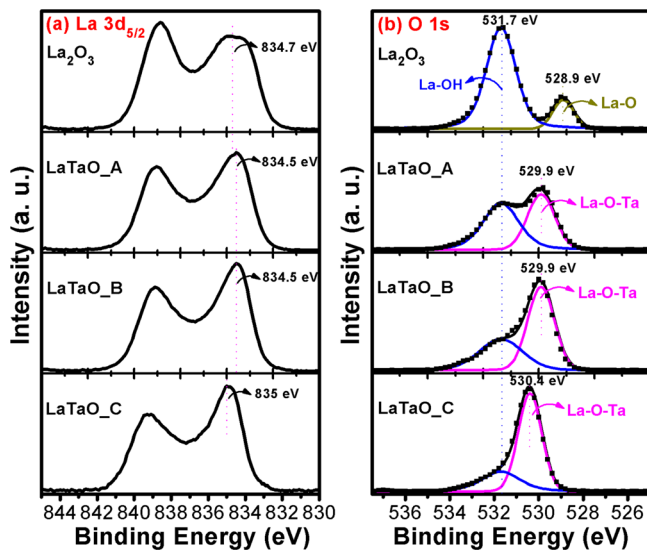


FIG. 1. XPS spectrum of (a) La  $3d_{5/2}$  and (b) O  $1s$  for the dielectric films in sample\_La<sub>2</sub>O<sub>3</sub>, sample\_LaTaO\_A, sample\_LaTaO\_B, and sample\_LaTaO\_C.

existence of La(OH)<sub>3</sub> in the La<sub>2</sub>O<sub>3</sub> film. With Ta incorporation, the La  $3d_{5/2}$  main peak becomes sharper, which is more obvious for higher Ta/(Ta + La) atomic ratio in the LaTaO film. This result is presumably due to the enhancement in the moisture resistance of the La<sub>2</sub>O<sub>3</sub> film and accordingly the suppression in the formation of La(OH)<sub>3</sub> after Ta incorporation. Nevertheless, the La  $3d_{5/2}$  peak related to sample\_LaTaO\_C (located at 835.0 eV) shifts to an even higher binding energy in comparison to sample\_La<sub>2</sub>O<sub>3</sub>, suggesting the formation of La-O-Ta bond in the LaTaO film. The O  $1s$  spectra of the La<sub>2</sub>O<sub>3</sub> and LaTaO films are shown in Fig. 1(b), and each

fitting peak follows the general shape of the Lorentzian–Gaussian function. As for the La<sub>2</sub>O<sub>3</sub> film, the two O  $1s$  peaks correspond to La-O bond (located at 528.9 eV)<sup>15</sup> and La-OH bond (located at 531.7 eV), respectively. Moreover, the O  $1s$  peak corresponding to La-O bond has a much higher intensity compared with that corresponding to La-OH bond, indicating that most of La atoms in the La<sub>2</sub>O<sub>3</sub> film have been transformed into La(OH)<sub>3</sub> due to moisture absorption. With Ta incorporation, the intensity of the O  $1s$  peak corresponding to La-OH bond decreases. Moreover, this effect becomes more obvious for higher Ta/(Ta + La) atomic ratio in the LaTaO film. This result further demonstrates the suppressed formation of La(OH)<sub>3</sub> due to the enhanced moisture resistance of the La<sub>2</sub>O<sub>3</sub> film after Ta incorporation. Meanwhile, the O  $1s$  peak corresponding to La-O bond has been completely replaced by that corresponding to La-O-Ta bond (located at a higher binding energy) for each Ta-incorporated sample. Moreover, the O  $1s$  peak corresponding to La-O-Ta bond shifts to a higher binding energy with increased Ta/(Ta + La) atomic ratio as reflected by the comparison between sample\_LaTaO\_C and the other two Ta-incorporated samples, and similar effect also occurs to the La  $3d_{5/2}$  spectrum in Fig. 1(a).

Fig. 2 shows the AFM images of the La<sub>2</sub>O<sub>3</sub> and LaTaO films with a measurement area of  $1 \mu\text{m} \times 1 \mu\text{m}$ . The La<sub>2</sub>O<sub>3</sub> film, with a RMS of 1.28 nm, exhibits the roughest surface among the dielectric films, which should result from non-uniform volume expansion of the La<sub>2</sub>O<sub>3</sub> film after moisture absorption.<sup>11</sup> With Ta incorporation, the dielectric roughness is significantly reduced, which is more obvious for higher Ta/(Ta + La) atomic ratio. Accordingly, the RMS value of LaTaO film in sample\_LaTaO\_A, sample\_LaTaO\_B, and

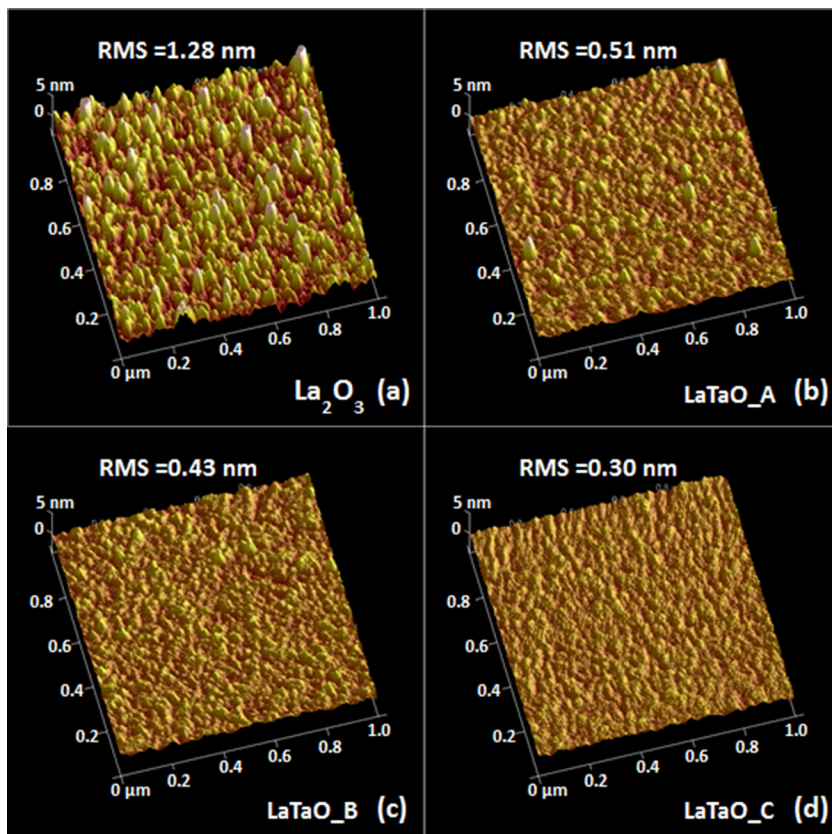


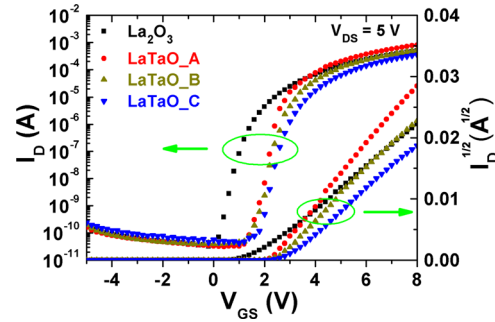
FIG. 2. AFM image of dielectric films in (a) sample\_La<sub>2</sub>O<sub>3</sub>, (b) sample\_LaTaO\_A, (c) sample\_LaTaO\_B, and (d) sample\_LaTaO\_C.

TABLE I. Extracted electrical parameters of the a-IGZO TFT's.

Sample	La <sub>2</sub> O <sub>3</sub>	LaTaO_A	LaTaO_B	LaTaO_C
La deposition (RF/W)	40	40	40	40
Ta deposition (DC/A)	0	0.03	0.04	0.05
Atomic ratio of Ta/(Ta + La)	0%	21.7%	30.6%	69.1%
$\mu_{\text{sat}}$ (cm <sup>2</sup> /V·s)	12.1	23.4	16.3	11.0
$V_{\text{TH}}$ (V)	1.85	2.40	2.66	2.97
SS (V/dec)	0.234	0.177	0.201	0.217
$\Delta V_{\text{H}}$ (V)	-0.76	0.10	1.29	2.34
$I_{\text{on}}$ ( $\mu\text{A}$ )	494	810	520	349
$I_{\text{on}}/I_{\text{off}}$	$1.5 \times 10^7$	$2.6 \times 10^7$	$1.3 \times 10^7$	$8.6 \times 10^6$
$C_{\text{ox}}$ ( $\mu\text{F}/\text{cm}^2$ )	0.231	0.262	0.269	0.279
Dielectric constant	10.4	11.8	12.2	12.6

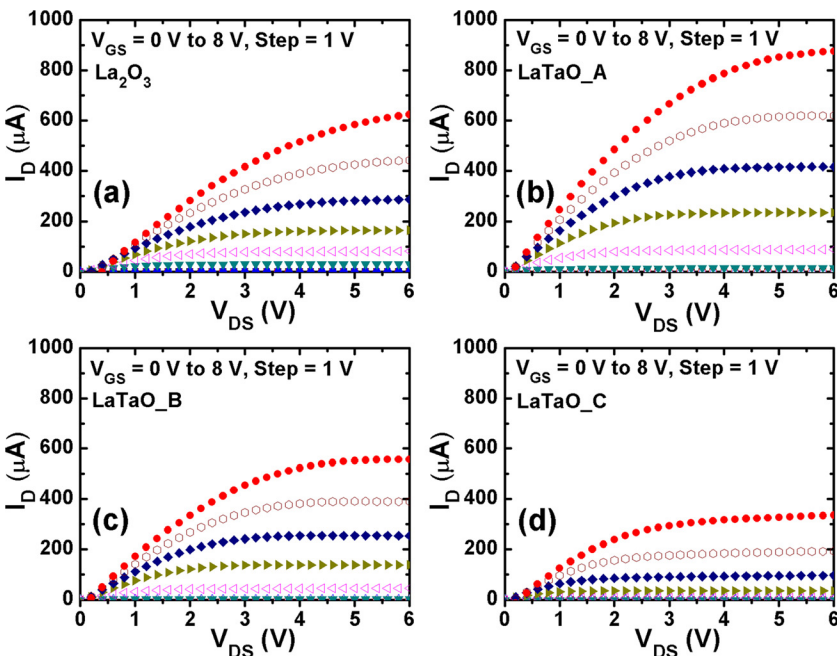
sample\_LaTaO\_C is 0.51 nm, 0.43 nm, and 0.30 nm, respectively, further demonstrating that Ta incorporation is an effective way to enhance the moisture resistance of La<sub>2</sub>O<sub>3</sub> film and accordingly reduce its surface roughness. In addition, the enhanced moisture resistance of the La<sub>2</sub>O<sub>3</sub> film also effectively suppresses the deterioration of its dielectric constant, and thus results in a continuous increase of dielectric constant associated with increasing Ta incorporation as listed in Table I. As compared to 3.9 of conventional SiO<sub>2</sub> dielectric, a larger dielectric constant of the LaTaO film ( $\sim 12$ ) is conducive to achieving higher-performance TFT with smaller operating voltage and larger output current.

Fig. 3 exhibits the transfer characteristics of the a-IGZO TFTs: drain current ( $I_{\text{D}}$ ) vs. gate-to-source voltage ( $V_{\text{GS}}$ ) and  $I_{\text{D}}^{1/2}$  vs.  $V_{\text{GS}}$  at a drain-to-source voltage ( $V_{\text{DS}}$ ) of 5 V. The saturation carrier mobility ( $\mu_{\text{sat}}$ ), threshold voltage ( $V_{\text{TH}}$ ), subthreshold swing (SS), on current ( $I_{\text{on}}$ ), and on-off current ratio ( $I_{\text{on}}/I_{\text{off}}$ ) of the devices are extracted from Fig. 3 and listed in Table I. Among them,  $\mu_{\text{sat}}$  and  $V_{\text{TH}}$  are calculated from a linear fitting to the plot of  $I_{\text{D}}^{1/2}$  versus  $V_{\text{GS}}$ , which is based on the I-V equation of field-effect transistor operating in the saturation region

FIG. 3. Transfer characteristics of the a-IGZO TFTs in sample\_La<sub>2</sub>O<sub>3</sub>, sample\_LaTaO\_A, sample\_LaTaO\_B, and sample\_LaTaO\_C.

$$I_{\text{D}} = (\mu_{\text{sat}} C_{\text{ox}} W / 2L) (V_{\text{GS}} - V_{\text{TH}})^2. \quad (1)$$

By comparing sample\_La<sub>2</sub>O<sub>3</sub> and sample\_LaTaO\_A,  $\mu_{\text{sat}}$  is nearly doubled from 12.1 cm<sup>2</sup>/V·s to 23.4 cm<sup>2</sup>/V·s with a reduction of SS from 0.234 V/dec to 0.177 V/dec due to the Ta incorporation in the La<sub>2</sub>O<sub>3</sub> gate dielectric. It is believed that the reduction in dielectric roughness can induce a smoother a-IGZO/dielectric interface, thus resulting in an increase in carrier mobility due to reduced surface-roughness scattering on the carriers.<sup>16</sup> In addition, carrier mobility can also be improved by reducing the trap density at/near the a-IGZO/dielectric interface because of the restraint of electron trapping. Hence, the increase in  $\mu_{\text{sat}}$  mentioned above can be attributed to smoother dielectric surface as well as lower trap density at/near the a-IGZO/dielectric interface, which are supported by the smaller values of RMS and SS, respectively.<sup>1,17</sup> Furthermore, it was reported that a large number of oxygen vacancies are easily generated in rare-earth oxide film due to the formation of hydroxide after reacting with moisture.<sup>18</sup> Hence, it is believed that the high trap density at/near the a-IGZO/dielectric interface in sample\_La<sub>2</sub>O<sub>3</sub> is related to the oxygen vacancies originated from the hygroscopicity of La<sub>2</sub>O<sub>3</sub>. In addition, a smaller  $V_{\text{TH}}$  (1.85 V) of sample\_La<sub>2</sub>O<sub>3</sub> in comparison to  $V_{\text{TH}}$  (2.40 V) of

FIG. 4. Output characteristics of the a-IGZO TFTs: (a) sample\_La<sub>2</sub>O<sub>3</sub>; (b) sample\_LaTaO\_A; (c) sample\_LaTaO\_B; and (d) sample\_LaTaO\_C.

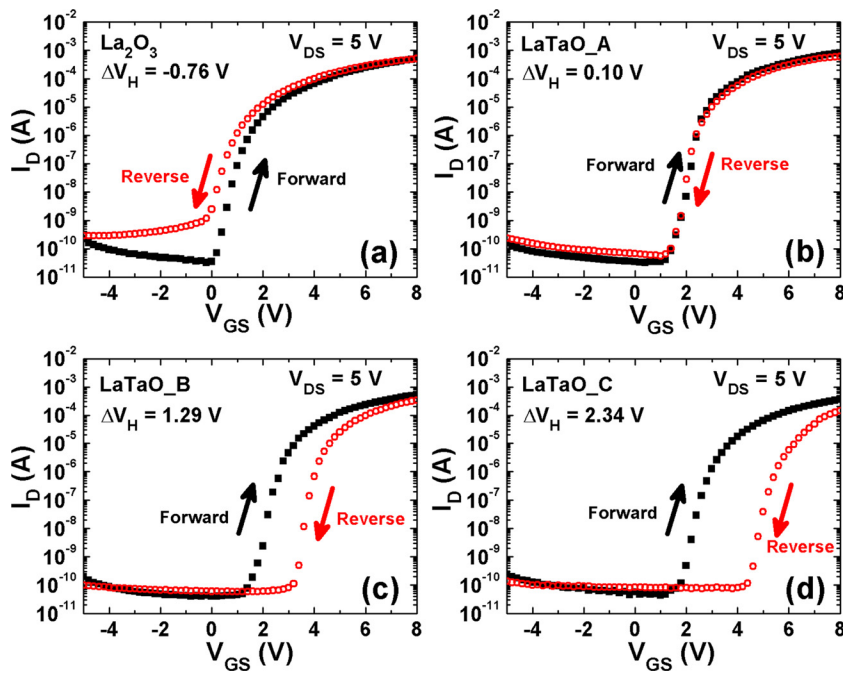


FIG. 5. Transfer characteristics of the a-IGZO TFTs measured under the forward and reverse  $V_{GS}$  sweepings: (a) sample\_La<sub>2</sub>O<sub>3</sub>; (b) sample\_LaTaO\_A; (c) sample\_LaTaO\_B; and (d) sample\_LaTaO\_C.

sample\_LaTaO\_A can further reveal the existence of oxygen vacancies in the La<sub>2</sub>O<sub>3</sub> gate dielectric as well as their reduction after Ta incorporation because oxygen vacancies can act as donor-like traps, inducing a negative shift of transfer curve and a degradation of SS in a-IGZO TFTs.<sup>19</sup> Besides,  $I_{on}$  and  $I_{on}/I_{off}$  are increased from 494  $\mu$ A and  $1.5 \times 10^7$  to 810  $\mu$ A and  $2.6 \times 10^7$ , respectively, by Ta incorporation due to the improvement in carrier mobility. However, for further increase of Ta incorporation in the gate dielectric, the electrical characteristics of the TFT start to degrade even with a smoother dielectric surface, as reflected by the results of sample\_LaTaO\_B and sample\_LaTaO\_C. This should be ascribed to the creation of new Ta-related traps because a high density of defect states generally exists in Ta<sub>2</sub>O<sub>5</sub> film,<sup>20</sup> which can be supported by the continual degradation of SS with increasing Ta/(Ta + La) atomic ratio in the LaTaO gate dielectric. Fig. 4 displays the output characteristics of the samples, which clearly exhibit an n-type enhancement mode. According to the comparison between sample\_La<sub>2</sub>O<sub>3</sub> and sample\_LaTaO\_A, the output current of the TFT is significantly increased by the Ta incorporation in the La<sub>2</sub>O<sub>3</sub> gate dielectric due to the increase in carrier mobility. A continual reduction in output current with increasing Ta/(Ta + La) atomic ratio in the LaTaO gate dielectric is observed, which is consistent with the degradation in SS due to the generation of new Ta-related traps.

As shown in Fig. 5, the hysteresis properties of the samples are investigated according to the transfer characteristics measured under forward and reverse  $V_{GS}$  sweepings successively.  $\Delta V_H$  is defined as the  $V_{TH}$  shift in the hysteresis loop. It is found that sample\_La<sub>2</sub>O<sub>3</sub> exhibits an obvious anticlockwise hysteresis with a negative  $\Delta V_H$  ( $-0.76$  V), further revealing the existence of donor-like traps at/near the a-IGZO/dielectric interface,<sup>21</sup> which is due to the introduction of oxygen vacancies in the La<sub>2</sub>O<sub>3</sub> film after moisture absorption. These donor-like traps can induce electron-detrapping or hole-trapping and become positively charged<sup>19</sup> during the forward  $V_{GS}$  sweep of the hysteresis measurement. As a result, a

decrease of  $V_{TH}$  is observed during the subsequent backward  $V_{GS}$  sweep. With Ta incorporation in the La<sub>2</sub>O<sub>3</sub> gate dielectric, negligible hysteresis is exhibited by sample\_LaTaO\_A ( $\Delta V_H = 0.10$  V), which further demonstrates the reduction in the trap density at/near the a-IGZO/dielectric interface due to the enhanced moisture resistance of the dielectric film and thus suppressed generation of oxygen vacancies. In addition, the generation of new Ta-related traps, which are acceptor-like and prefer to capture electrons, has also been revealed by the continual enhancement of clockwise hysteresis with increasing Ta/(Ta + La) atomic ratio in the LaTaO gate dielectric. As a result, larger  $\Delta V_H$  is exhibited by sample\_LaTaO\_B ( $\Delta V_H = 1.29$  V) and sample\_LaTaO\_C ( $\Delta V_H = 2.34$  V). A similar phenomenon of different signs of  $\Delta V_H$  for hysteresis related to donor-like and acceptor-like traps has also been observed in other work.<sup>22</sup>

In this work, the impact of Ta incorporation in La<sub>2</sub>O<sub>3</sub> gate dielectric on the electrical characteristics of a-IGZO TFT has been studied. It is found that Ta incorporation can effectively enhance the moisture resistance of the La<sub>2</sub>O<sub>3</sub> film and suppress the formation of La(OH)<sub>3</sub>, thus reducing the dielectric roughness as well as the trap density at/near the a-IGZO/dielectric interface. Accordingly, the electrical characteristics of the TFT are significantly improved as reflected by nearly doubled  $\mu_{sat}$ , reduced SS, suppressed hysteresis, and increased output current. However, excessive incorporation of Ta in the gate dielectric can degrade the device characteristics due to the creation of new Ta-related traps. In summary, these results demonstrate the potential use of LaTaO gate dielectric for making high-performance a-IGZO TFTs.

This work was supported by the University Development Fund (Nanotechnology Research Institute, 00600009) of the University of Hong Kong.

<sup>1</sup>J. S. Park, W. J. Maeng, H. S. Kim, and J. S. Park, *Thin Solid Films* **520**, 1679 (2012).

- <sup>2</sup>T. Kamiya, K. Nomura, and H. Hosono, *Sci. Technol. Adv. Mater.* **11**, 044305 (2010).
- <sup>3</sup>R. A. Street, *Adv. Mater.* **21**, 2007 (2009).
- <sup>4</sup>L. F. Deng, P. T. Lai, W. B. Chen, J. P. Xu, Y. R. Liu, H. W. Choi, and C. M. Che, *IEEE Electron Dev. Lett.* **32**, 93 (2011).
- <sup>5</sup>H. Yabuta, M. Sano, K. Abe, T. Aiba, T. Den, H. Kumomi, K. Nomura, T. Kamiya, and H. Hosono, *Appl. Phys. Lett.* **89**, 112123 (2006).
- <sup>6</sup>K. Nomura, H. Ohta, A. Takagi, T. Kamiya, M. Hirano, and H. Hosono, *Nature* **432**, 488 (2004).
- <sup>7</sup>J. S. Lee, S. Chang, S. M. Koo, and S. Y. Lee, *IEEE Electron Dev. Lett.* **31**, 225 (2010).
- <sup>8</sup>J. B. Kim, C. F. Hernandez, and B. Kippelen, *Appl. Phys. Lett.* **93**, 242111 (2008).
- <sup>9</sup>J. Robertson, *Eur. Phys. J. Appl. Phys.* **28**, 265 (2004).
- <sup>10</sup>C. H. Kao, H. Chen, J. S. Chiu, K. S. Chen, and Y. T. Pan, *Appl. Phys. Lett.* **96**, 112901 (2010).
- <sup>11</sup>Y. Zhao, M. Toyama, K. Kita, K. Kyuno, and A. Toriumi, *Appl. Phys. Lett.* **88**, 072904 (2006).
- <sup>12</sup>Y. J. Jo, I. H. Lee, and J. S. Kwak, *Mater. Res. Bull.* **47**, 2919 (2012).
- <sup>13</sup>Y. Zhao, K. Kita, K. Kyuno, and A. Toriumi, *Appl. Phys. Lett.* **89**, 252905 (2006).
- <sup>14</sup>S. C. Sun and T. F. Chen, *IEEE Trans. Electron Dev.* **44**, 1027 (1997).
- <sup>15</sup>T. L. Barr, *J. Phys. Chem.* **82**, 1801 (1978).
- <sup>16</sup>P. K. Nayak, M. N. Hedhili, D. Cha, and H. N. Alshareef, *Appl. Phys. Lett.* **100**, 202106 (2012).
- <sup>17</sup>J. K. Jeong, J. H. Jeong, H. W. Yang, J. S. Park, Y. G. Mo, and H. D. Kim, *Appl. Phys. Lett.* **91**, 113505 (2007).
- <sup>18</sup>F. H. Chen, J. L. Her, S. Mondal, M. N. Hung, and T. M. Pan, *Appl. Phys. Lett.* **102**, 193515 (2013).
- <sup>19</sup>X. Xiao, W. Deng, S. Chi, Y. Shao, X. He, L. Wang, and S. Zhang, *IEEE Trans. Electron Dev.* **60**, 4159 (2013).
- <sup>20</sup>S. Huang, *IEEE Trans. Electron Dev.* **60**, 2741 (2013).
- <sup>21</sup>C. T. Tsai, T. C. Chang, S. C. Chen, I. Lo, S. W. Tsao, M. C. Hung, J. J. Chang, C. Y. Wu, and C. Y. Huang, *Appl. Phys. Lett.* **96**, 242105 (2010).
- <sup>22</sup>L. X. Qian and P. T. Lai, *IEEE Trans. Dev. Mater. Reliab.* **14**, 177 (2014).